

This is the author's final version of the contribution published as:

ALK, ROS1, and NTRK Rearrangements in Metastatic Colorectal Cancer

Pietrantonio F*, **Di Nicolantonio F***, Schrock AB, Lee J, Tejpar S, Sartore-Bianchi A, Hechtman JF, Christiansen J, Novara L, Tebbutt N, Fucà G, Antoniotti C, Kim ST, Murphy D, Berenato R, Morano F, Sun J, Min B, Stephens PJ, Chen M, Lazzari L, Miller VA, Shoemaker R, Amatu A, Milione M, Ross JS, Siena S, Bardelli A, Ali SM, Falcone A, de Braud F, Cremolini C.

J Natl Cancer Inst. 2017 Dec 1;109(12). doi: 10.1093/jnci/djx089.

*corresponding authors

The publisher's version is available at:

<https://academic.oup.com/jnci/article-abstract/109/12/djx089/3860155>

When citing, please refer to the published version.

Link to this full text:

<http://hdl.handle.net/>

This full text was downloaded from iris-AperTO: <https://iris.unito.it/>

ALK, ROS1 and NTRK rearrangements define a new subtype of metastatic colorectal cancer

^{1#}Filippo Pietrantonio, ^{2,3#}Federica Di Nicolantonio, ⁴Alexa B. Schrock, ⁵Jeeyun Lee, ⁶Sabine Tejpar, ⁷Andrea Sartore-Bianchi, ⁸Jaclyn F. Hechtman, ⁹Jason Christiansen, ³Luca Novara, ¹⁰Niall Tebbutt, ¹Giovanni Fucà, ^{11,12}Carlotta Antoniotti, ⁵Seung Tae Kim, ⁹Danielle Murphy, ¹Rosa Berenato, ¹Federica Morano, ⁴James Sun, ⁹Bosun Min, ⁴Philip J. Stephens, ⁹Marissa Chen, ^{2,3}Luca Lazzari, ⁴Vincent A. Miller, ⁹Robert Shoemaker, ⁷Alessio Amatu, ¹³Massimo Milione, ¹⁴Jeffrey S. Ross, ^{7,15}Salvatore Siena, ^{2,3}Alberto Bardelli, ⁴Siraj M. Ali, ^{11,12}Alfredo Falcone, ^{1,15}Filippo de Braud and ^{11,12}Chiara Cremolini

Authors' affiliations:

- 1- Medical Oncology Department, Fondazione IRCCS Istituto Nazionale dei Tumori, Milan, Italy
- 2- Department of Oncology, University of Torino, 10060 Candiolo (TO), Italy;
- 3- Candiolo Cancer Institute-FPO, IRCCS, 10060 Candiolo (TO), Italy;
- 4- Foundation Medicine, Inc., Cambridge, Massachusetts;
- 5- Samsung Medical Center, Sungkyunkwan University School of Medicine, Kangnamgu, Seoul, Korea;
- 6- Molecular Digestive Oncology Unit, University Hospital Gasthuisberg, Leuven, Belgium;
- 7- Niguarda Cancer Center, Grande Ospedale Metropolitano Niguarda, Milan, Italy.
- 8- Memorial Sloan Kettering Cancer Center, New York, NY
- 9- Ignyta Inc., San Diego, CA
- 10- Austin Health, Melbourne VIC, Australia
- 11- Azienda Ospedaliero-Universitaria Pisana, Pisa, Italy
- 12- University of Pisa, Pisa, Italy
- 13- Department of Diagnostic Pathology and Laboratory Medicine, Fondazione IRCCS Istituto Nazionale dei Tumori, Milan, Italy;
- 14- Department of Pathology, Albany Medical College, Albany, NY
- 15- Department of Oncology and Hemato-oncology, Università degli Studi di Milano, Milan, Italy.

Drs. Pietrantonio and Di Nicolantonio contributed equally to this article

* To whom correspondence should be addressed:

Dr Filippo Pietrantonio,
Department of Medical Oncology, Medical Oncology Unit,
Fondazione IRCCS Istituto Nazionale dei Tumori,
Via Venezian 1, 20133 Milan, Italy
Phone: + 39-0223903807
E-mail: filippo.pietrantonio@istitutotumori.mi.it

Dr Federica Di Nicolantonio
Department of Oncology, University of Torino
Strada Provinciale 142, Km 3.95
10060 Candiolo, Torino, Italy
Phone: +39-011-9933523
Fax: +39-011-9933225
E-mail: federica.dinicolantonio@unito.it

Acknowledgment of research support for the study:

This work was supported by Fondazione ARCO (Associazione Ricerche e Cure in Oncologia), Italy and partly supported by grants AIRC IG n. 17707 (F.D.N.); AIRC IG n. 16788 (A.B.); Fondo per la Ricerca Locale (ex 60%), Università di Torino, 2014 (F.D.N.); and grant Fondazione Piemontese per la Ricerca sul Cancro-ONLUS 5 per mille 2011 Ministero della Salute (A.B.). Investigators at Niguarda Cancer Center are supported by the following grants: Terapia Molecolare dei Tumori (A.S-B, S. S.) and Dynamic of Tumor Evolution & Therapy (A. S-B) from Fondazione Oncologia Niguarda Onlus; Associazione Italiana per la Ricerca sul Cancro (AIRC) 2010 Special Program Molecular Clinical Oncology 5x1000, project 9970 (S.S., A.B.). European Community's grant agreement no. 635342-2 MoTriColor (A.B., S.S.).

The Authors would like to thank Fabio Picchini for graphical support.

Running head: *ALK*, *ROS1* and *NTRK* rearranged metastatic colorectal cancer

Number of tables/figures: 5

Abstract

Background: *ALK*, *ROS1* and *NTRK* fusions occur in 0.2%-2.4% of colorectal cancers. Pioneer cases of mCRC patients bearing rearrangements who benefited from anti-ALK, ROS, TrkA-B-C therapies were reported.

Methods: Clinical features, molecular characteristics and outcome of 27 mCRC patients bearing *ALK*, *ROS1*, *NTRK* rearranged tumors were compared with those of a cohort of 319 patients not bearing rearrangements. Deep molecular and immunophenotypic characterizations of rearranged cases, including those described in the TCGA database, were performed.

Results: Closely recalling the “*BRAF* history”, *ALK*, *ROS1* and *NTRK* rearrangements more frequently occurred in elderly patients ($p=0.024$) with right-sided ($p<0.001$) and node-spreading ($p=0.03$), *RAS* wild-type ($p<0.001$), MSI-high ($p<0.001$) cancers. All patients bearing *ALK*, *ROS1*, and *NTRK* fusions had shorter overall survival (15.6 months) than negative patients (33.7 months), both in the univariate (HR 2.17, 95%CI 1.03-4.57; $p<0.001$) and multivariate models (HR 2.78, 95%CI 1.27-6.07; $p=0.011$). All four evaluable patients with rearrangements showed primary resistance to anti-EGFRs. Frequent association with potentially targetable *RNF43* mutations was observed in MSI-high rearranged tumors.

Conclusion: *ALK*, *ROS1*, *NTRK* rearrangements define a new rare subtype of mCRC with extremely poor prognosis. Primary tumor site, MSI-high, *RAS* and *BRAF* status may help to identify patients bearing these alterations. While sensitivity to available treatments is limited, targeted strategies inhibiting ALK, ROS and TrkA-B-C provided encouraging results.

Genomic translocations leading to the constitutive activation of receptor tyrosine kinases (RTKs) play a crucial role in tumorigenesis across different malignancies, including colorectal cancer (CRC) ^{1,2}. RTK fusions involving *ALK*, *ROS1*, and *NTRK1-2-3* (*NTRK*) occur in 0.2%-2.4% of CRCs ^{3,4}, and may represent new targets for therapeutic intervention ⁵⁻¹⁷. Addition to kinase suppression or pharmacological inhibition has been reported in CRC preclinical models bearing RTK fusions, including the *TPM3-NTRK1* rearranged KM12 cell line ¹⁸, the *ALK* rearranged cell line C10 ¹⁹, patient-derived primary cell lines ¹⁰ and patient-derived xenografts ²⁰. So far, a single heavily pre-treated metastatic CRC (mCRC) patient whose tumor bore an *LMNA-NTRK1* fusion was treated with entrectinib, an oral selective inhibitor of *ALK*, *ROS1*, and TrkA-B-C (the protein products of the *NTRK1-2-3* genes, respectively), with clinical benefit ¹⁵. Another mCRC patient whose tumor harbored *STRN-ALK* fusion received the oral *ALK* inhibitor ceritinib and achieved response ¹⁶, and a patient with a *CAD-ALK* rearrangement responded to entrectinib ⁶.

Despite these pioneer case reports, it has not been clearly established whether *ALK*, *ROS1*, or *NTRK* rearranged tumors represent a distinct, although rare, disease subtype that should be detected early in order to adopt a tailored management strategy that may include targeted treatments.

Although a few reports have described the occurrence of *ALK*, *ROS1* and *NTRK* fusions in CRC (Supplementary Table 1), there is still limited knowledge about clinical and pathological characteristics, prognosis and sensitivity of these tumors to available treatments including anti-EGFR monoclonal antibodies (MoAbs) such as cetuximab and panitumumab. Similarly, except for some preclinical reports ^{11,19}, comprehensive molecular and functional data to clarify whether these alterations confer oncogene addiction and to suggest perspectives on optimal treatment strategies are not available yet.

We therefore carried out a global effort aimed at characterizing the molecular and clinical landscape of *ALK*, *ROS1* and *NTRK* rearranged mCRCs. Even though a broader list of gene fusions has been described in CRC, including those affecting *RET*, *HER2* and *BRAF* ^{2,8,22,23}, we specifically focused

on mCRC with *ALK*, *ROS1* and *NTRK* rearrangements since their phylogeny is closely related and they are frequently grouped as targets of newly developed agents such as entrectinib ²⁴.

Methods

Study design and participants

In the clinical step (Figure 1), the cohort of 319 *ALK*, *ROS1* and *NTRK* negative cases included patients screened for Ignyta's phase 1 program at: Samsung Medical Center (SMC), Seoul, South Korea (n=209); Azienda Ospedaliero-Universitaria Pisana (AOUP), Pisa, Italy (n=79); Fondazione IRCCS Istituto Nazionale dei Tumori (INT), Milan, Italy (n=31). The population of 27 *ALK*, *ROS1*, *NTRK* rearranged mCRCs included patients collected at: Foundation Medicine Inc. (FMI), Cambridge, Massachusetts (n=12); Samsung Medical Center (SMC), Seoul, South Korea (n=4); Memorial Sloan Kettering Cancer Center (MSKCC), NYC, New York (n=3); Austin Health, Heidelberg, Australia (n=3) on behalf of MAX trial Investigators; Fondazione IRCCS Istituto Nazionale dei Tumori (INT), Milan, Italy (n=2); Niguarda Cancer Center (NCC), Milan, Italy (n=2); University Hospital Gasthuisberg (UHG), Leuven, Belgium (n=1). Molecular screening methods are detailed as Supplementary Methods and summarized in Figure 1. Study participants signed a written informed consent and the study was approved by the Institutional Review Board of INT, Milan.

Statistical analysis

We investigated the association of *ALK*, *ROS1* and *NTRK* rearrangements with the following variables collected at the diagnosis of mCRC: age, gender, ECOG performance status (0, ≥ 1), primary tumor location (right colon, left colon, rectum), primary tumor resection, mucinous histology, time to metastases (synchronous, metachronous), number of metastatic sites (1, >1), metastatic sites (lung, lymph nodes, liver, peritoneum), *RAS* and *BRAF* status (mutated, wild-type),

MMR status (proficient, deficient). Fisher's exact test, χ^2 test or Mann-Whitney tests were used when appropriate to assess the associations of the *ALK*, *ROS1*, *NTRK* rearrangements with investigated characteristics. Statistical significance was set at $p=0.05$ for a bilateral test.

We investigated the impact of *ALK*, *ROS1* and *NTRK* rearrangements on overall survival (OS), defined as the time from diagnosis of metastatic disease to death or last follow up for alive patients. OS analysis was determined according to the Kaplan-Meier method and survival curves were compared using the log-rank test. The correlation of *ALK*, *ROS1*, *NTRK* status and clinicopathological characteristics with OS was assessed in univariate analysis. In order to minimize the bias of multiple comparisons, according to the false discovery rate correction, statistical significance was set at $p=0.009$ for a bilateral test. Cox proportional hazard model was adopted in the multivariate analysis, including as covariates variables correlated with survival with $p<0.1$ in the univariate analyses. Hazards' proportionality was assumed.

All analyses were carried out by means of Prism 7 for Mac OS X v7.0.

Translational analyses

As shown in Figure 1 and Supplementary Methods, NGS data were obtained through 3 different panels: FMI panel in 15 cases, Minerva panel (Ignyta Inc.®) in 11 cases, MSK-IMPACT panel in 1 case. The association of individual samples with the type of translocation identified and NGS panel is shown in Supplementary Table 2. Finally, analysis in silico from TCGA data was performed (Supplementary Methods).

Results

Study population

Based on a systematic literature review, we identified 24 published cases of *ALK*, *ROS1* or *NTRK* rearranged CRCs (Supplementary Table 1). Nineteen were staged as metastatic, and informative medical records were retrieved for fifteen of them. Taking advantage of screening programs

worldwide, we were able to identify 12 additional cases. Therefore, the final population consisted of 27 *ALK*, *ROS1*, *NTRK* rearranged mCRCs (Figure 1; Supplementary Table 2) including a newly described *SCYL3-NTRK1* fusion (Supplementary Figure 1). We compared the clinical and pathological features of *ALK*, *ROS1*, and *NTRK* rearranged mCRCs with a cohort of *ALK*, *ROS1*, and *NTRK* negative patients (n=319), screened for phase 1 studies at three Institutions (Figure 1). The overall incidence of *ALK*, *ROS1*, or *NTRK* rearrangements at these Institutions was 1,5% (5 out of 324 screened samples).

Clinical and pathological features of ALK, ROS1 and NTRK rearranged mCRC

As shown in Table 1, rearrangements were more frequent in older patients (p=0.024) with right-sided tumors (80.0% vs 30.0%; p<0.001), and spread more frequently to lymph nodes (45.8% vs 24.7%; p= 0.030) and less frequently to the liver (41.7% vs 65.5%; p=0.026). Additionally, although only 50% of patients in the control group had available information on MSI status, a higher percentage of tumors bearing rearrangements were MSI-high (48.1% vs 8.1%; p<0.001).

Of note, *RAS* mutations were much less frequent in rearranged than in other tumors (7.4% vs 48.3%; p<0.001). Only one (3.7%) rearranged sample showed the co-occurrence of *SLC34A2-ROS1* fusion and *BRAF* V600E mutation. Overall, right-sided primary location, *RAS* wild-type and MSI-high status, in addition to female gender, were particularly associated with *NTRK* rearrangements. Notably, patients with right-sided, *RAS* and *BRAF* wild-type, MSI-high mCRCs had 54- and 453-fold higher chances of harboring *ALK*, *ROS1*, or *NTRK* rearrangements (OR=54.0, 95% CI: 13.3-219.1; p<0.001) or specifically *NTRK* rearrangements (OR=453.0, 95% CI: 67.2-3053.4; p<0.001), respectively. These four easy to collect characteristics (primary tumor site, MSI, *RAS* and *BRAF* status) enable identification of patients bearing an *ALK*, *ROS1*, or *NTRK* rearrangement with positive and negative predictive values of 75% and 95%. The positive and negative predictive values with specific regard to *NTRK* rearrangements were 75% and 99%.

Molecular features of ALK, ROS1 and NTRK rearranged CRC

Molecular reports from next-generation sequencing DNA analyses performed on rearranged cases were retrieved (Figure 1). Additionally, molecularly annotated genomic variants from seven CRC samples harboring *ALK* or *NTRK3* fusions (Supplementary Figure 2 and 3) in the TCGA database were gathered. First, we focused on the subset of genes previously reported as the most frequently mutated in CRCs (Figure 2A) ²³. In line with previous reports regarding MSI-high BRAF mutated CRC ²⁴⁻²⁶, MSI-high rearranged tumors were enriched for alterations affecting *RNF43* (64.7% vs 5.9%; p=0.0004 Fisher's exact test), most of which were frameshift changes affecting glycine 659, which lies within a mononucleotide repeat (Figure 2A).

A low prevalence of *RAS/BRAF* mutations, also accounting for MSI-high status (Figure 2B), was reported. Only one MSS rearranged tumor displayed a BRAF V600E mutation, while two MSI-high rearranged mCRC samples carried *BRAF* alterations (I371M and K475R) of unknown significance and two MSS rearranged CRCs showed a well-established oncogenic variant (G469A), and an alteration (D594H) that impairs BRAF kinase activity but paradoxically activates MEK and ERK through transactivation of CRAF, respectively. The prevalence of *PIK3CA* mutations in CRCs carrying rearrangements (12.1%) did not significantly differ from what reported in unselected colorectal tumors ²³.

An explorative analysis of selected genes implicated in immune-escape mechanisms ²⁷ was conducted by retrieving the transcriptomic profiles of the seven rearranged samples for which RNA seq data was available from the TCGA and these were compared with non rearranged MSI-high CRC samples also from TCGA (Figure 2C). Although the analysis suggested that the presence of rearrangements did not impact the typical MSI-high phenotype represented by the upregulation of immunoinhibitory molecules ²⁷, the small number of samples limits the power of this observation.

Prognostic impact of ALK, ROS1 and NTRK rearrangements in mCRC

Finally, we explored the clinical impact of *ALK*, *ROS1* and *NTRK* rearrangements in the metastatic setting (TCGA samples were excluded from survival analyses, since they were mostly found in earlier disease stages and had incomplete follow-up data). When looking at OS results, at a median

follow-up of 28.5 months [95%CI 23.8-36.9], patients bearing *ALK*, *ROS1* or *NTRK* rearranged tumors had poor prognosis when compared with rearrangement negative tumors (median OS: 15.6 [95%CI 10.0-20.4] versus 33.7 [95%CI 28.3-42.1] months; HR for death: 2.17, 95% CI 1.03-4.57; $p < 0.001$) (Figure 3A). When applying the false discovery rate correction, the association of *ALK*, *ROS1* and *NTRK* rearrangements with OS was still statistically significant ($p < 0.005$). In the multivariable model (Table 2) including other covariates associated with OS with $p < 0.1$ (age, primary tumor location, primary resection, *BRAF* mutation and MSI status), the presence of gene rearrangements was still associated with shorter OS [HR for death: 2.33, 95% CI 1.10-4.95; $p = 0.020$]. Notably, patients with *ALK*, *ROS1* or *NTRK* rearranged tumors had short OS independently from MSI status (Figure 3B). In fact, median OS was 17.0 (95% CI 10.0-31.4) months for patients with MSS rearranged tumors and 15.6 (95% CI 10.0-20.4) months for MSI-high ones. Moreover, the poor prognostic impact of gene rearrangements was independent of primary tumor location: both in right- and left-sided tumors patients bearing rearrangements had shorter OS than those with negative tumors (Supplementary Figure 4).

Therapeutic implications of ALK, ROS1 and NTRK rearrangements in mCRC

All the patients with rearranged tumors that were treated with cetuximab or panitumumab (N=4) experienced disease progression as best response during the treatment with anti-EGFR agents (Supplementary Methods; Supplementary Figure 5).

One patient with *EML4-ALK* rearrangement and MSI-high tumor received single agent anti-PD-1 treatment with nivolumab and achieved a durable response (Supplementary Figure 5). Notably, the IHC staining of this tumor revealed intense staining for CD4, CD8, CD68 and especially PDL-1, with an abundant intra and extratumoral lymphocytic infiltration (Supplementary Figure 6).

Discussion

Here we showed that *ALK*, *ROS1* and *NTRK* rearrangements identify an uncommon CRC molecular subtype with specific clinical, pathological and molecular features. The investigated fusions (and particularly those affecting *NTRK*) were more frequent in elderly females with right-sided tumors, spreading to extra-regional lymph nodes. However, the most clinically relevant association was found with MSI-high and *RAS* wild-type status, which are two relevant and commonly used biomarkers for patient selection for immunotherapy and anti-EGFRs, respectively. This type of clinical and molecular associations resemble very closely what observed for codon 600 *BRAF* mutations and, interestingly, *BRAF* V600 mutations and gene fusions were almost invariably mutually exclusive. Since MSI-high status is reported in less than 5% of mCRCs²⁸, the frequency of MSI-high rearranged tumors is unexpectedly high (48.1%), even considering the right-sided location²⁹. The frequency of MSI-high status in *ALK*, *ROS1* and *NTRK* rearranged tumors seems similar or even higher than in *BRAF* V600E mutated mCRCs, where it reaches 30-35%^{24,28}. While the association between right-sided tumors, MSI-high and *BRAF* mutations is well established, we report for the first time a strong association with right-sided tumor location and MSI-high status also for gene fusions. Of note, while frame-shift mutations occurring in MSI-high cancers are heterogeneously represented in tumor sub-clones³⁰, gene rearrangements appear as “founder” events, as they are present in most, if not all, tumor cells. Nevertheless, since defective mismatch repair is also an early event in CRC carcinogenesis, the adenoma-carcinoma sequence should be further elucidated for this rare subtype. Future studies exploring the role of food carcinogens and/or peculiar microbiota components in the right colon are also warranted to clarify the potential link between MSI status and kinase rearrangements.

When compared with negative samples, *ALK*, *ROS1*, and *NTRK* rearranged tumors show a low frequency of *RAS* and *BRAF* oncogenic mutations. A low prevalence of *BRAF* V600E mutation was reported in the group of negative tumors (5.8%), probably as a consequence of the poor

prognosis and rapid progression of *BRAF* mutant tumors, preventing these patients to receive later lines of therapy and therefore to be screened for phase 1 trials. Therefore, we were unable to identify a statistically significant difference in terms of *BRAF* mutations between rearranged and not rearranged tumors ($p=1.000$) in the present series. However, the observation that *ALK*, *ROS1* and *NTRK* rearrangements co-occur rarely with other common driver events in the RTK-RAS pathway, and specifically *RAS* and *BRAF* codon 600 mutations, supports the hypothesis that gene fusions drive oncogene addiction. Indeed, previous reports indicate that *NTRK1* and *ALK* rearranged CRC preclinical models and patients respond to pharmacological blockade of the fusion kinase^{6,11,15,19,20}. In spite of the relatively low prevalence of gene fusions, the identification of patients with tumors bearing these alterations may be simplified and enriched by the evaluation of four simple and easy-to-collect variables (i.e. primary tumor location, *RAS*, *BRAF* and MSI-high status), which are available for the vast majority of patients. Therefore, in an evidence-based perspective of resource sparing, the molecular screening for gene rearrangements should not be denied to patients with *RAS* and *BRAF* wild-type and/or MSI-high mCRC.

A high prevalence of *RNF43* frameshift mutations was reported among *ALK*, *ROS1* and *NTRK* rearranged tumors, though in the absence of concomitant *BRAF* V600E mutations, thus suggesting that gene rearrangements may act as driver events alternative to *BRAF* in the tumorigenesis of MSI-high right-sided tumors carrying *RNF43* alterations. Since porcupine inhibitors are being developed to suppress paracrine WNT-driven growth of *RNF43* mutant tumors (<https://clinicaltrials.gov/ct2/show/NCT02278133>), our findings may provide a rationale for co-targeting tyrosine kinase oncogenic fusions as well as the WNT pathway in this rare tumor subset.

Closely recalling the long “*BRAF* history”, we found that gene fusions occurring in mCRCs are associated with unfavorable outcome. However, it must be pointed out that patients with MSI-high mCRCs have worse OS independently from the co-occurrence of *BRAF* V600E mutation²⁸. Therefore, given the association of *ALK*, *ROS1* or *NTRK* rearrangements with MSI-high status and the mutual exclusivity with codon 600 *BRAF* mutations, our findings may partly explain the

aggressive behaviour of MSI-high *BRAF* wild-type mCRCs. The same observations are true for the potential contribution of gene fusion to the poor prognosis of some right-sided mCRCs ³¹.

Again, consistent with previous findings regarding *BRAF* V600E mutations ³², *ALK*, *ROS* and *NTRK* rearranged tumors seem not to derive benefit from anti-EGFR monoclonal antibodies, thus confirming preclinical observations ¹⁹. Given the very low frequency of gene fusions in mCRC, the validation of this finding is quite unrealistic. However, these results are supported by a strong biologic rationale and may contribute to explain – at least in part - the limited activity of anti-EGFRs in right-sided, *RAS* and *BRAF* wild-type tumors ³³. From a clinical perspective, it seems therefore reasonable to offer an intensive first-line regimen, such as the triplet FOLFOXIRI plus bevacizumab to patients with right-sided, *ALK*, *ROS1*, and *NTRK* rearranged mCRCs ³⁴, based on their aggressive behaviour, and in line with current recommendations for *BRAF* V600E mutant tumors.

Our observations argue that the early enrolment of patients with tumors bearing *ALK*, *ROS1* and *NTRK* rearrangements in clinical trials with matched targeted agents should be highly encouraged, as this subset of patients may in fact be uniquely poised to benefit from targeted strategies.

Nevertheless, benefit from targeted strategies against *ALK*, *ROS1*, and *TrkA-B-C* may be transient and mechanisms of acquired resistance may occur early ^{17,20}. This is quite reasonable particularly when considering the impressive mutational burden of MSI-high tumors that may promote in these tumors the early emergence of acquired resistance.

The combination of targeted agents and immunotherapy approaches in MSI-high rearranged tumors may be a promising strategy to be further investigated, supported by a strong molecular rationale, and by the absence of impact of rearrangements on MSI-high associated immunophenotype.

The major limitation of this study is the choice of the control group. Although a wider series of negative cases, especially those analyzed by MSK-IMPACT or FoundationOne tests, would have been more appropriate, both MSK-IMPACT and FoundationOne are DNA-based assays and do not

completely cover intronic regions, thus making possible to miss some gene fusions. Moreover, clinical data were not available for the vast majority of these patients. Therefore, a cohort of well-annotated patients screened at three Institutions for a phase 1 trial and quite representative of the general population of mCRC patients was adopted as control group.

In conclusion, the features of *ALK*, *ROS1* and *NTRK* rearrangements are somewhat reminiscent of the peculiar traits previously recognized in *BRAF* V600E mutant mCRC. These fusions define a new molecular subtype of mCRC associated with poor prognosis, whose recognition allows a proper tailored management for a new subgroup of patients. The large-scale diffusion of this assessment may be eased by the availability of a multi-step procedure for the detection of gene fusions, starting from a simple IHC test with high sensitivity, or a comprehensive approach able to identify *ALK*, *ROS1*, and *NTRK* rearrangements, as well as other potentially targetable kinase fusions²². Finally, while the poor prognosis of rearranged tumors may suggest the adoption of upfront intensive treatments when feasible, new targeted strategies are under investigation and the high prevalence of MSI-high status in rearranged tumors opens the way to evaluate new combination approaches, including targeted (ALK, ROS1, TrkA-B-C) and immunotherapy agents.

References

1. Shaw, A.T., Hsu, P.P., Awad, M.M. & Engelman, J.A. Tyrosine kinase gene rearrangements in epithelial malignancies. *Nat Rev Cancer* **13**, 772-787 (2013).
2. Stransky, N., Cerami, E., Schalm, S., Kim, J.L. & Lengauer, C. The landscape of kinase fusions in cancer. *Nat Commun* **5**, 4846 (2014).
3. Amatu, A., Sartore-Bianchi, A. & Siena, S. NTRK gene fusions as novel targets of cancer therapy across multiple tumour types. *ESMO Open* **1**(2016).
4. Rankin, A., *et al.* Broad Detection of Alterations Predicted to Confer Lack of Benefit From EGFR Antibodies or Sensitivity to Targeted Therapy in Advanced Colorectal Cancer. *Oncologist* (2016).
5. Aisner, D.L., *et al.* ROS1 and ALK fusions in colorectal cancer, with evidence of intratumoral heterogeneity for molecular drivers. *Mol Cancer Res* **12**, 111-118 (2014).
6. Amatu, A., *et al.* Novel CAD-ALK gene rearrangement is drugable by entrectinib in colorectal cancer. *Br J Cancer* **113**, 1730-1734 (2015).
7. Creancier, L., *et al.* Chromosomal rearrangements involving the NTRK1 gene in colorectal carcinoma. *Cancer Lett* **365**, 107-111 (2015).
8. Hechtman, J.F., *et al.* Identification of Targetable Kinase Alterations in Patients with Colorectal Carcinoma That are Preferentially Associated with Wild-Type RAS/RAF. *Mol Cancer Res* **14**, 296-301 (2016).
9. Houang, M., *et al.* ALK and ROS1 overexpression is very rare in colorectal adenocarcinoma. *Appl Immunohistochem Mol Morphol* **23**, 134-138 (2015).
10. Lee, J., *et al.* Detection of novel and potentially actionable anaplastic lymphoma kinase (ALK) rearrangement in colorectal adenocarcinoma by immunohistochemistry screening. *Oncotarget* **6**, 24320-24332 (2015).
11. Lee, S.J., *et al.* NTRK1 rearrangement in colorectal cancer patients: evidence for actionable target using patient-derived tumor cell line. *Oncotarget* **6**, 39028-39035 (2015).
12. Lin, E., *et al.* Exon array profiling detects EML4-ALK fusion in breast, colorectal, and non-small cell lung cancers. *Mol Cancer Res* **7**, 1466-1476 (2009).
13. Lipson, D., *et al.* Identification of new ALK and RET gene fusions from colorectal and lung cancer biopsies. *Nat Med* **18**, 382-384 (2012).
14. Park do, Y., *et al.* NTRK1 fusions for the therapeutic intervention of Korean patients with colon cancer. *Oncotarget* **7**, 8399-8412 (2016).
15. Sartore-Bianchi, A., *et al.* Sensitivity to Entrectinib Associated With a Novel LMNA-NTRK1 Gene Fusion in Metastatic Colorectal Cancer. *J Natl Cancer Inst* **108**(2016).
16. Yakirevich, E., *et al.* Oncogenic ALK Fusion in Rare and Aggressive Subtype of Colorectal Adenocarcinoma as a Potential Therapeutic Target. *Clin Cancer Res* **22**, 3831-3840 (2016).
17. Drilon, A., *et al.* Safety and Antitumor Activity of the Multi-Targeted Pan-TRK, ROS1, and ALK Inhibitor Entrectinib (RXDX-101): Combined Results from Two Phase 1 Trials (ALKA-372-001 and STARTRK-1). *Cancer Discov.* (2017).
18. Ardini, E., *et al.* The TPM3-NTRK1 rearrangement is a recurring event in colorectal carcinoma and is associated with tumor sensitivity to TRKA kinase inhibition. *Mol Oncol* **8**, 1495-1507 (2014).
19. Medico, E., *et al.* The molecular landscape of colorectal cancer cell lines unveils clinically actionable kinase targets. *Nat Commun* **6**(2015).
20. Russo, M., *et al.* Acquired Resistance to the TRK Inhibitor Entrectinib in Colorectal Cancer. *Cancer Discov.* **6**, 36-44 (2016).
21. Le Rolle, A.F., *et al.* Identification and characterization of RET fusions in advanced colorectal cancer. *Oncotarget* **6**, 28929-28937 (2015).
22. Ross, J.S., *et al.* The distribution of BRAF gene fusions in solid tumors and response to targeted therapy. *Int J Cancer* **138**, 881-890 (2016).
23. Network, T.C.G.A. Comprehensive molecular characterization of human colon and rectal cancer. *Nature* **487**, 330-337 (2012).

24. Giannakis, M., *et al.* Genomic Correlates of Immune-Cell Infiltrates in Colorectal Carcinoma. *Cell Rep* (2016).
25. Giannakis, M., *et al.* RNF43 is frequently mutated in colorectal and endometrial cancers. *Nature Genetics* **46**, 1264-1266 (2014).
26. Yan, H.H., *et al.* RNF43 germline and somatic mutation in serrated neoplasia pathway and its association with BRAF mutation. *Gut* (2016).
27. Angelova, M., *et al.* Characterization of the immunophenotypes and antigenomes of colorectal cancers reveals distinct tumor escape mechanisms and novel targets for immunotherapy. *Genome Biol* **16**, 64 (2015).
28. Venderbosch S, Nagtegaal ID, Maughan TS, *et al.* Mismatch repair status and BRAF mutation status in metastatic colorectal cancer patients: a pooled analysis of the CAIRO, CAIRO2, COIN, and FOCUS studies. *Clin Cancer Res* 2014; **20**: 5322-30.
29. Yamauchi M, Morikawa T, Kuchiba A, *et al.* Assessment of colorectal cancer molecular features along bowel subsites challenges the conception of distinct dichotomy of proximal versus distal colorectum. *Gut* 2012; **61**: 847-54.
30. Williams, MJ, Werner B, Barnes CP, Graham TA, Sottoriva A. Identification of neutral tumor evolution across cancer types. *Nature Genetics* 2016; **48**: 238-44.
31. Petrelli F, Tomasello G, Borgonovo K, *et al.* Prognostic Survival Associated With Left-Sided vs Right-Sided Colon Cancer: A Systematic Review and Meta-analysis. *JAMA Oncol.* 2016 Oct 27. doi: 10.1001/jamaoncol.2016.4227. [Epub ahead of print]
32. Pietrantonio F, Petrelli F, Coinu A, *et al.* Predictive role of BRAF mutations in patients with advanced colorectal cancer receiving cetuximab and panitumumab: A meta-analysis. *Eur. J. Cancer* 2015; **51**: 587-94.
33. Moretto R, Cremolini C, Rossini D, *et al.* Location of Primary Tumor and Benefit From Anti-Epidermal Growth Factor Receptor Monoclonal Antibodies in Patients With RAS and BRAF Wild-Type Metastatic Colorectal Cancer. *Oncologist* 2016; **21**: 988-94.
34. Cremolini C, Loupakis F, Antoniotti C, *et al.* FOLFOXIRI plus bevacizumab versus FOLFIRI plus bevacizumab as first-line treatment of patients with metastatic colorectal cancer: updated overall survival and molecular subgroup analyses of the open-label, phase 3 TRIBE study. *Lancet Oncol* 2015; **16**: 1306-15.

Table 1. Patients' characteristics according to the presence or absence of *ALK*, *ROS1*, *NTRK* rearrangements, or specifically for presence or absence of *NTRK* and *ALK* rearrangements.

| Characteristics | | <i>ALK</i> , <i>ROS1</i> , <i>NTRK</i> | <i>ALK</i> , <i>ROS1</i> , <i>NTRK</i> | <i>p</i> * | <i>NTRK</i> | <i>p</i> † | <i>ALK</i> | <i>p</i> ‡ |
|-------------------------------|-------------|--|--|------------------|-------------------------------|------------------|-------------------------------|--------------|
| | | negative (N=319) N (%) | rearranged (N=27) N (%) | | rearranged (N=13) N (%) | | rearranged (N=11) N (%) | |
| Sex | Female | 129 (40.4) | 18 (66.7) | 0.159 | 9 (69.2) | 0.047 | 7 (63.6) | 0.211 |
| | Male | 190 (59.6) | 9 (33.3) | | 4 (30.8) | | 4 (36.4) | |
| Age | Median | 57 | 64 | 0.024 | 68 | 0.032 | 55 | 0.967 |
| | Range | 15-88 | 40-62 | | 33-73 | | 40-87 | |
| ECOG PS | 0 | 106 (33.4) | 9 (64.3) | 0.250 | 2 (25.0) | 1.000 | 3 (75.0) | 0.115 |
| | 1-2 | 211 (66.6) | 5 (35.7) | | 6 (75.0) | | 1 (25.0) | |
| | NA | 2 | 13 | | 5 | | 7 | |
| Primary tumor location | Right colon | 98 (31.0) | 20 (80.0) | <0.001 | 10 (90.9) | <0.001 | 8 (72.7) | 0.014 |
| | Left colon | 125 (39.6) | 3 (12.0) | | 0 | | 2 (18.2) | |
| | Rectum | 93 (29.4) | 2 (8.0) | | 1 (9.1) | | 1 (9.1) | |
| | NA | 3 | 2 | | 2 | | 0 | |
| Mucinous histology | Yes | 40 (12.7) | 1 (5.9) | 0.706 | 0 | 0.602 | 1 (11.1) | |

| | | | | | | | | |
|-----------------------------------|--------------|------------|-----------|-------|------------|-------|-----------|--------|
| | No | 276 (87.3) | 16 (94.1) | | 8 (100.0) | | 8 (88.9) | 1.000 |
| | NA | 3 | 10 | | 5 | | 2 | |
| Primary tumor resected | Yes | 240 (75.2) | 19 (86.4) | | 8 (72.7) | | 0 | |
| | No | 79 (24.8) | 3 (13.6) | 0.308 | 3 (27.3) | 1.000 | 8 (100.0) | <0.001 |
| | NA | 0 | 5 | | 2 | | 3 | |
| Time to metastases | Synchronous | 210 (66.2) | 11 (64.7) | | 5 (62.5) | | 6 (75.0) | |
| | Metachronous | 107 (33.8) | 6 (35.3) | 1.000 | 3 (37.5) | 1.000 | 2 (25.0) | 0.723 |
| | NA | 2 | 10 | | 5 | | 3 | |
| Number of metastatic sites | 1 | 161 (50.9) | 14 (58.3) | | 7 (63.6) | | 6 (54.5) | |
| | >1 | 155 (49.1) | 10 (41.7) | 0.531 | 4 (36.4) | 0.544 | 5 (45.5) | 1.000 |
| | NA | 3 | 3 | | 2 | | 0 | |
| Lung metastases | Yes | 129 (40.8) | 5 (20.8) | | 0 | | 4 (36.4) | |
| | No | 187 (59.2) | 19 (79.2) | 0.053 | 11 (100.0) | 1.000 | 7 (63.6) | 1.000 |
| | NA | 3 | 3 | | 2 | | 0 | |
| Lymph Nodes metastases | Yes | 78 (24.7) | 11 (45.8) | | 7 (63.6) | | 3 (27.3) | |
| | No | 238 (75.3) | 13 (54.2) | 0.030 | 4 (36.4) | 0.008 | 8 (72.7) | 0.737 |
| | NA | 3 | 3 | | 2 | | 0 | |
| Liver metastases | Yes | 207 (65.5) | 10 (41.7) | | 4 (36.4) | | 5 (45.5) | |
| | No | 109 (34.5) | 14 (58.3) | 0.026 | 7 (63.6) | 0.058 | 6 (54.5) | 0.204 |

| | | | | | | | | |
|--|---------------|------------|-----------|--------|------------|--------|------------|--------|
| | NA | 3 | 3 | | 2 | | 0 | |
| Peritoneal metastases | Yes | 89 (28.2) | 8 (33.3) | | 5 (45.5) | | 3 (27.3) | |
| | No | 227 (71.8) | 16 (66.7) | 0.640 | 6 (54.5) | 0.306 | 8 (72.7) | 1.000 |
| | NA | 3 | 3 | | 2 | | 0 | |
| RAS status | wild-type | 155 (51.7) | 25 (92.6) | | 11 (84.6) | | 9 (81.8) | |
| | mutated | 145 (48.3) | 2 (7.4) | <0.001 | 2 (15.4) | <0.001 | 2 (18.2) | 0.065 |
| | NA | 19 | 0 | | 0 | | 0 | |
| BRAF status | wild-type | 258 (94.2) | 26 (96.3) | | 13 (100.0) | | 11 (100.0) | |
| | V600E mutated | 16 (5.8) | 1 (3.7) | 1.000 | 0 | 1.000 | 0 | 1.000 |
| | NA | 45 | 0 | | 0 | | 0 | |
| MSI status | MSS | 148 (91.9) | 14 (51.9) | | 3 (23.1) | | 4 (36.4) | |
| | MSI-high | 13 (8.1) | 13 (48.1) | <0.001 | 10 (76.9) | <0.001 | 7 (63.6) | <0.001 |
| | NA | 158 | 0 | | 0 | | 0 | |
| NA: not available. *Comparison of <i>ALK</i> , <i>ROS1</i> , <i>NTRK</i> rearranged versus not rearranged tumors; †Comparison of <i>NTRK</i> rearranged versus not rearranged tumors; ‡Comparison of <i>ALK</i> rearranged versus not rearranged tumors. <i>ROS1</i> rearranged tumors were not separately analyzed because of the small sample size (N=3) | | | | | | | | |

Table 2. Association of *ALK*, *ROS*, *NTRK* rearrangements and known prognostic baseline characteristics with OS

| Characteristics | | N | Univariate analyses | | | Multivariable model | | |
|--|-------------------|-----|---------------------|-----------|------------------|---------------------|-----------|------------------|
| | | | HR | 95% CI | <i>p</i> | HR | 95% CI | <i>p</i> |
| <i>ALK</i> , <i>ROS</i> , <i>NTRK</i> status | Negative | 316 | 1 | - | - | 1 | - | - |
| | Rearranged | 20 | 2.17 | 1.03-4.57 | <0.001 | 2.33 | 1.10-4.95 | 0.020 |
| Age | - | 336 | 1.04 | 1.02-1.05 | <0.001 | 1.04 | 1.02-1.07 | <0.001 |
| ECOG PS | 0 | 112 | 1 | - | - | - | - | - |
| | 1-2 | 216 | 1.01 | 0.72-1.42 | 0.950 | - | - | - |
| Primary tumor site | Left colon/Rectum | 221 | 1 | - | - | 1 | - | - |
| | Right colon | 113 | 1.41 | 1.01-2.00 | 0.038 | 1.11 | 0.62-1.98 | 0.733 |
| Mucinous histology | No | 290 | 1 | - | - | - | - | - |
| | Yes | 41 | 0.97 | 0.59-1.58 | 0.885 | - | - | - |
| Primary resection | Yes | 257 | 1 | - | - | 1 | - | - |
| | No | 82 | 1.51 | 1.01-2.29 | 0.024 | 1.69 | 0.94-3.05 | 0.079 |
| Time to metastases | Metachronous | 113 | 1 | - | - | - | - | - |
| | Synchronous | 220 | 1.24 | 0.88-1.74 | 0.242 | - | - | - |
| Number of metastatic sites | 1 | 171 | 1 | - | - | - | - | - |
| | >1 | 164 | 1.28 | 0.93-1.77 | 0.134 | - | - | - |
| <i>RAS</i> status | Wild-type | 173 | 1 | - | - | - | - | - |
| | Mutated | 147 | 1.31 | 0.94-1.82 | 0.117 | - | - | - |
| <i>BRAF</i> status | Wild-type | 275 | 1 | - | - | 1 | - | - |
| | Mutated | 17 | 2.20 | 0.97-4.95 | 0.058 | 0.91 | 0.35-2.38 | 0.855 |
| MSI status | MSS | 156 | 1 | - | - | 1 | - | - |
| | MSI-high | 22 | 2.28 | 1.09-4.76 | 0.005 | 1.42 | 0.63-3.21 | 0.397 |

Figure Legends

Figure 1. Study flow-chart.

Top: A total of 27 metastatic colorectal cancer (mCRC) cases with *ALK* (n=11), *ROS1* (n=3) and *NTRK* (n=13) translocations were collected. Patients were retrieved by: Ignyta's phase 1 screening program in Italy, Belgium and South Korea; MAX trial's post-hoc analysis conducted in Australia; Foundation Medicine Inc. (FMI) dataset in USA; Memorial Sloan Kettering-Integrated Mutation Profiling of Actionable Cancer Targets (MSK-IMPACT) screening program in USA. **Bottom left:** Clinicopathological characteristics, *RAS* and *BRAF* status, Mismatch-repair (MMR) status, survival and treatment outcome data in the *ALK*, *ROS1*, *NTRK* rearranged population (n=27) were compared with those from a cohort of *ALK*, *ROS1*, *NTRK* negative mCRC patients (n=319) included in Ignyta's phase 1 screening program. **Bottom right:** Annotated genetic variants were retrieved from targeted next-generation sequencing analyses of tumor samples (N=27) from *ALK*, *ROS1*, *NTRK* rearranged mCRC patients. The number of samples analyzed by different gene panels is shown. Analysis of publicly available RNA sequencing data from the TCGA COADREAD (colorectal) study allowed the identification of 7 additional tumors carrying *ALK* or *NTRK3* translocations. Molecular annotations from TCGA translocated tumors were pooled with those from mCRC patients to increase power of detecting genetic alterations co-existing with *ALK*, *ROS1*, *NTRK* rearrangements.

Figure 2. Molecular profile of *ALK*, *ROS1*, *NTRK* rearranged colorectal cancer. **A.** OncoPrint map depicting alterations in top mutated colorectal cancer genes in *ALK*, *ROS1*, *NTRK* rearranged cancers (27 cases from this study and 7 samples from TCGA²³). Individual sample cases are designated by columns (top) and grouped by MMR status, while individual genes are presented by rows. **B.** Gene mutation profiles, excluding silent mutations, were compared between *ALK*, *ROS1*, *NTRK* rearranged cancers (27 cases from this study and 7 samples from TCGA) and data previously reported in a large-scale sequencing study of unselected CRC²⁵. Grey bars indicate the number of samples that were not sequenced for the indicated genes. **C.** Expression (RNA sequencing data) of selected genes implicated in immunoevasion (gene list was obtained from²⁵) in *ALK* or *NTRK3* rearranged tumors identified in TCGA, grouped based on their MMR status. The average expression of non-rearranged TCGA MSI-high CRC samples (n=92) from TCGA is also shown.

Figure 3. Survival in metastatic colorectal cancer patients carrying *ALK*, *ROS1*, *NTRK* rearranged tumors. **Panel A:** Kaplan-Meier curves for overall survival (OS) in patients with *ALK*, *ROS1*, *NTRK* rearrangements (n=20; red line) as compared to those with *ALK*, *ROS1*, *NTRK* negative tumors (n=316; blue line). **Panel B:** Kaplan-Meier curves for overall survival (OS) in patients with *ALK*, *ROS1*, *NTRK* rearrangements and MMR proficient status (n=11; red line) or patients with *ALK*, *ROS1*, *NTRK* rearrangements and MMR deficient status (n=9; green line) as compared to those with *ALK*, *ROS1*, *NTRK* negative tumors (n=316; blue line).

Contributors

Study design: FP, FDN, CC

Data collection and patients' recruitment: FP, FDN, GF, CA, STK, DM, JS, BM, PJS, MC, LL, VAM, RS, RB, FM, AA, CC

Data analysis and interpretation: FP, FDN, ABS, JL, ST, ASB, JH, JC, LN, NT, MM, JSR, SS, AB, SMA, AF, FDB, CC

Manuscript writing: all authors

Manuscript revision and approval: all authors

Declaration of interests

F.P. is a consultant/advisory board member for Roche, Amgen, Eli-Lilly, Bayer, Sanofi. S.S. is an advisory board member for Amgen, Roche, Novartis, Eli-Lilly, Bayer, Sanofi, Merck, Merrimack.

A.B. is a member of advisory boards for Horizon Discovery and Trovogene. A.F. is a consultant/advisory board member for Bayer, Roche, Amgen, Eli-Lilly, Merck Serono, Sanofi, Servier. F.d.B. is a consultant/advisory board member for Roche, Amgen, Novartis, Celgene, Boehringer-Ingelheim. C.C. is a consultant/advisory board member for Roche, Amgen, Eli-Lilly, Bayer, Merck Serono.

A.B.S., J.S., P.J.S., V.A.M., J.S.R., and S.M.A. are employees and have equity interest in Foundation Medicine, Inc. J.C., D.M., B.M., M.C., R.S. are employees and have equity interest in Ignyta, Inc

All other authors declare no potential competing interests

Figure 1

A

| | <i>NTRK</i> fusions N=13 | <i>ALK</i> fusions N=11 | <i>ROS1</i> fusions N=3 |
|---|--|---|--|
| Ignity's STARTRK-1 phase 1 study screening program † | <i>LMNA-NTRK1</i> (n=1) [7] <i>TPM3-NTRK1</i> (n=3*) [8] <i>SCYL3-NTRK1</i> (n=1*) | <i>CAD-ALK</i> (n=1) [9] <i>EML4-ALK</i> (n=2*) [6] | |
| MAX trial post-hoc analysis ‡ | | <i>EML4-ALK</i> (n=1) [4] | <i>Unknown-ROS1</i> (n=1) [4] <i>SLC34A2-ROS1</i> (n=1) [4] |
| Foundation Medicine Inc, Clinical database | <i>TPM3-NTRK1</i> (n=4*) <i>ETV6-NTRK3</i> (n=2) [12] <i>LMNA-NTRK1</i> (n=1*) | <i>CAD-ALK</i> (n=2*) [6] <i>EML4-ALK</i> (n=1) [11] <i>CENPF-ALK</i> (n=1) [11] <i>PRKAR1B-ALK</i> (n=1) [11] <i>MAPRE3-ALK</i> (n=1) [11] <i>STRN-ALK</i> (n=1) [11] | <i>GOPC-ROS1</i> (n=1*) |
| MSK-IMPACT screening program | <i>LMNA-NTRK1</i> (n=1*) | | |



***ALK, ROS, NTRK* rearranged mCRCs
N=27**



B

Clinicopathological characteristics available, N=27
RAS, BRAF status available, N=27
 MMR status available, N=26
 Survival data available, N=20
 Treatment data available, N=14



***ALK, ROS, NTRK* negative mCRCs
N= 319**

C

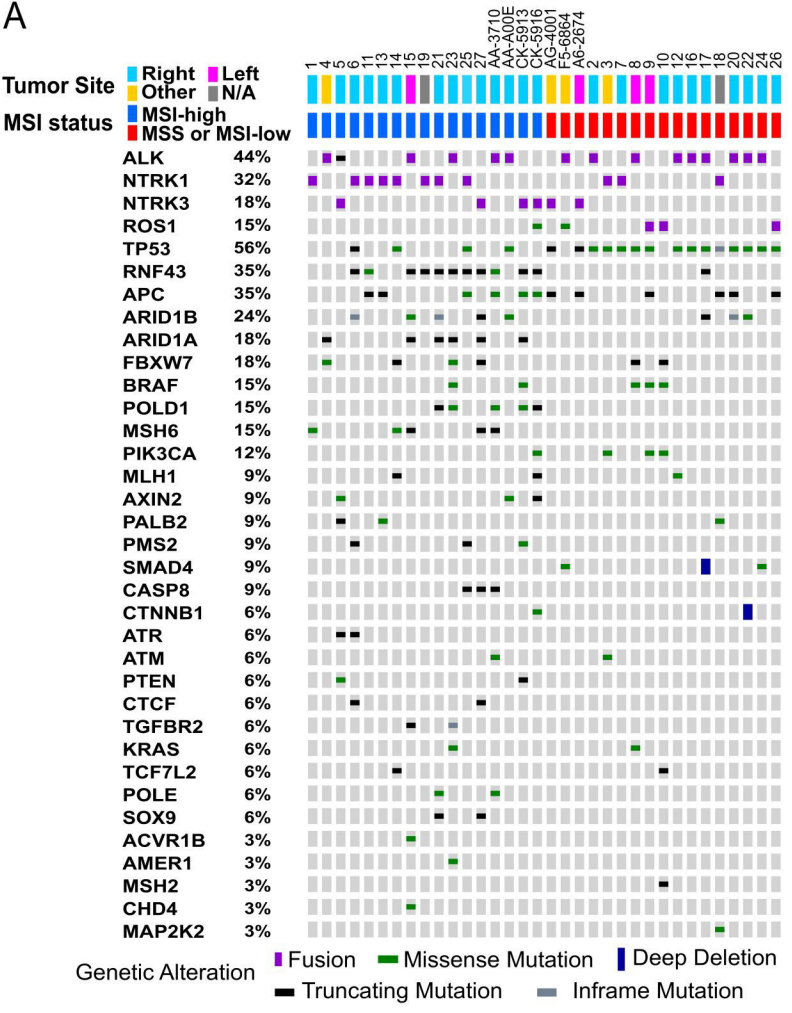
NGS data available N=27, by means of:

- Minerva panel, N= 11
- Foundation Medicine Inc. (FMI) panel, N= 15
- MSK-IMPACT, N=1

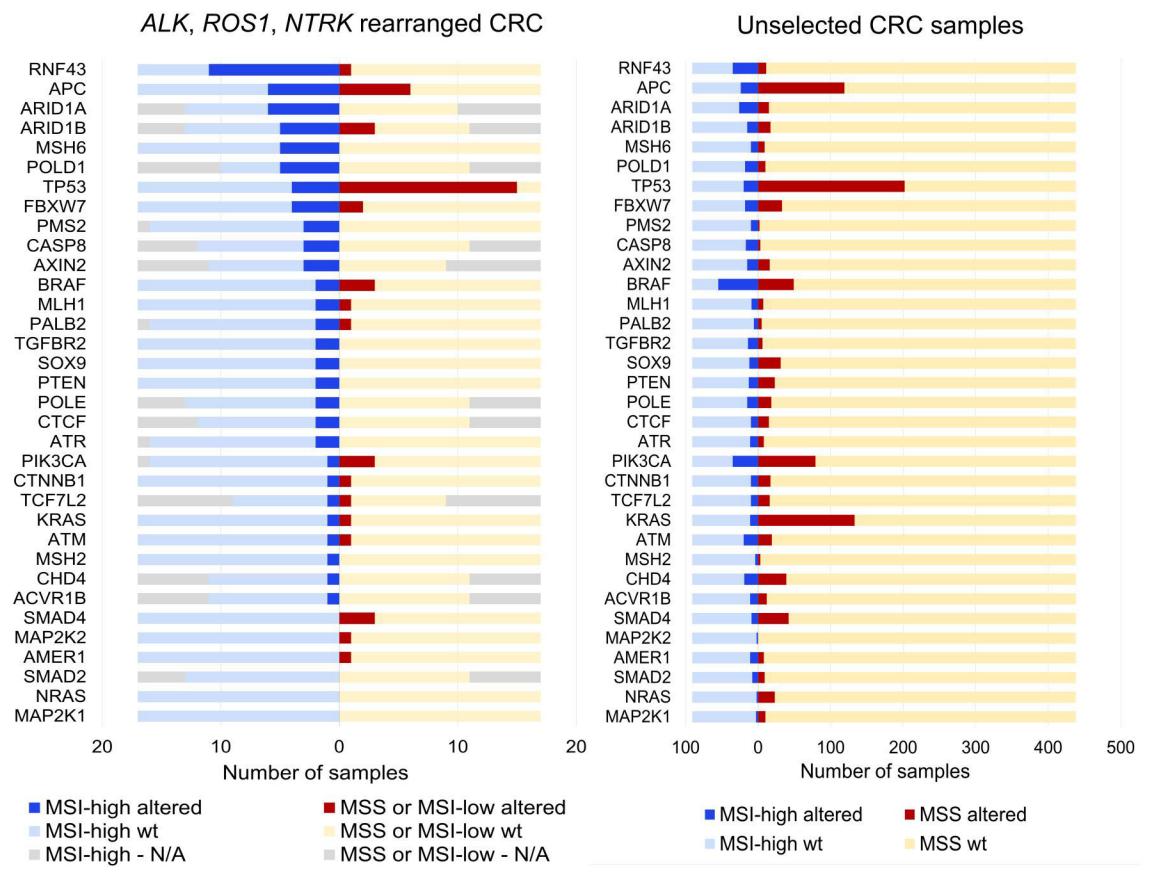
+
ALK, NTRK rearranged CRC samples in TCGA
 N= 7

Figure 2

A



B



C

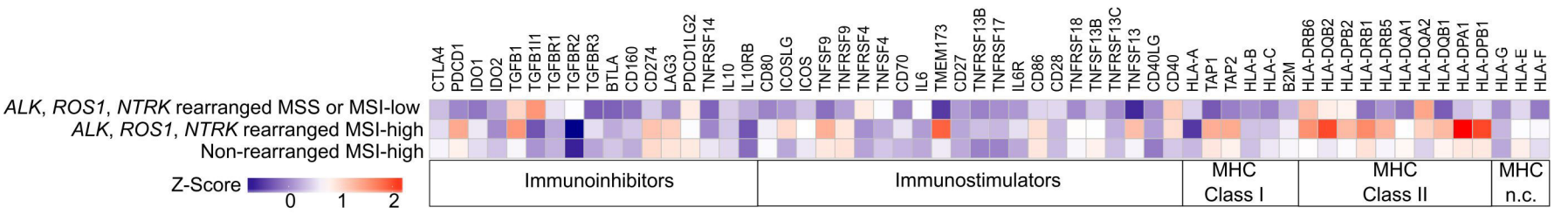
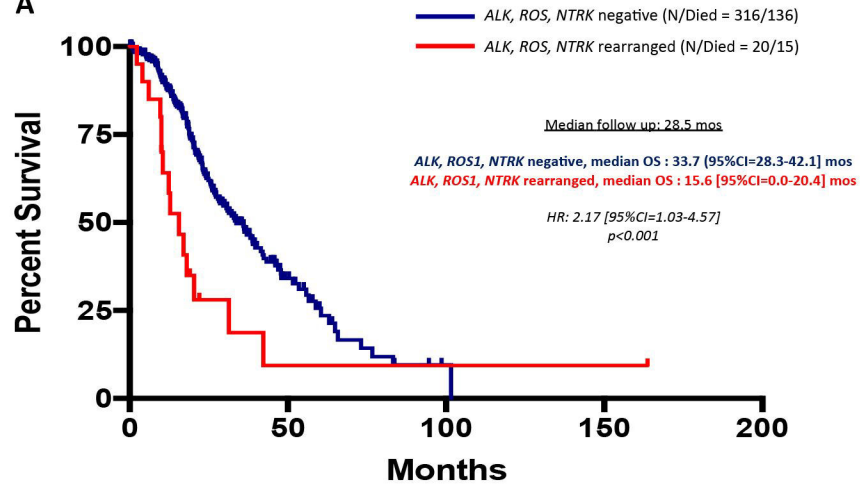


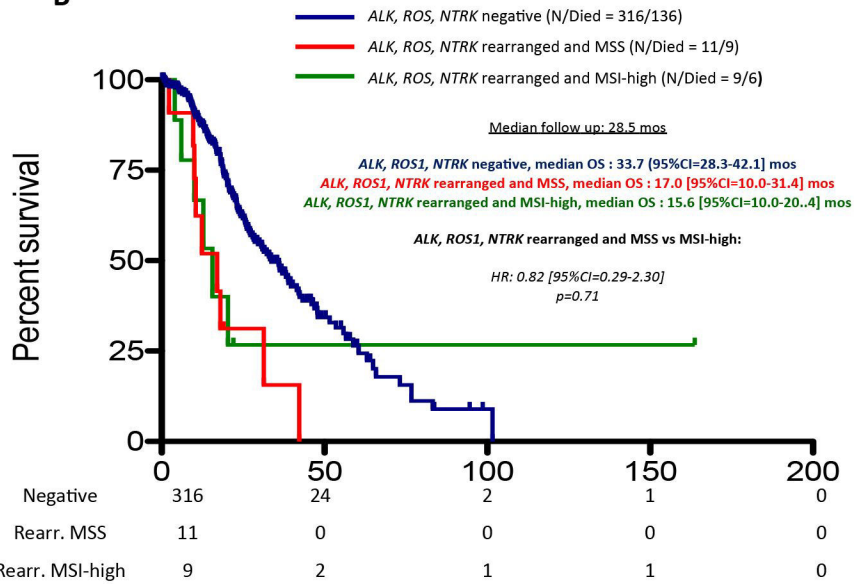
Figure 3

A



| | | | | | |
|------------|-----|----|---|---|---|
| Negative | 316 | 24 | 2 | 1 | 0 |
| Rearranged | 20 | 2 | 1 | 1 | 0 |

B



| | | | | | |
|-----------------|-----|----|---|---|---|
| Negative | 316 | 24 | 2 | 1 | 0 |
| Rearr. MSS | 11 | 0 | 0 | 0 | 0 |
| Rearr. MSI-high | 9 | 2 | 1 | 1 | 0 |

Supplementary Material

Supplement to: Pietrantonio F, Di Nicolantonio F, Schrock et al. *ALK, ROS1 and NTRK rearrangements define a new subtype of metastatic colorectal cancer*

Contents

Supplementary Methods

Supplementary Table 1

Supplementary Table 2

Supplemental Figure 1

Supplemental Figure 2

Supplemental Figure 3

Supplemental Figure 4

Supplemental Figure 5

Supplementary References

Supplementary Methods

Patients screening and translational analyses

1 - STARTRK1 phase 1 study by Ignyta®. In the first step, all screened samples were submitted to Immunohistochemistry (IHC) staining, as previously described ¹. Briefly, a cocktail of antibodies targeted to the C-terminal domains of pan-Trk (including TrkA, TrkB, TrkC, Cell Signaling, clone C17F1, 1:25 dilution), ROS1 (Cell Signaling, clone D4D6, 1:500 dilution) and ALK (Cell Signaling, clone D5F3, 1:500 dilution) was used with a single diaminobenzidine (DAB) reporter system. The presence of staining indicates the elevation of expression for at least one of the proteins targeted by the antibody cocktail. In the second step, all samples scored positive for IHC staining were tested by RNA-based next generation sequencing to determine the presence/absence of a gene fusion. The presence and nature of gene rearrangements/fusions was determined by RNA sequencing using a method previously described ¹. Total nucleic acid (a combination of both DNA and RNA) was isolated from FFPE tissues (Agencourt, Beckman) and sequencing libraries were generated using an anchored multiplex PCR (AMP) method ^{1,2}. RNA quality and amplifiable ability of the extracted material was assessed as previously described ¹. Briefly, the PreSeq RNA QC assay, which uses qPCR analysis of the housekeeping gene, VCP was performed on all samples. The RNA quality assessment was used to determine the potential for a false negative result from specimens where the RNA was fragmented to a degree that a gene rearrangement could not be amplified or mapped reliably. Sequencing was performed on the Illumina MiSeqDx platform (Illumina, San Diego, CA).

For patients screened at Ignyta, DNA next generation sequencing (NGS) analysis was performed through the custom “Minerva” panel, which interrogated 263 genes resumed in the list below:

| | | | | | | | | | |
|---------|-------|--------|--------|-------|-------|--------|--------|---------|--------|
| ABL1 | BRIP1 | CHEK2 | ERG | GLI1 | IHH | MET | NTF4 | RUNX1 | TSC2 |
| AKT1 | BTC | CHMP2A | ESR1 | GNA11 | IKZF1 | MIB1 | NTRK1 | RUNX1T1 | TYRO3 |
| AKT2 | BTK | CREBBP | EZH2 | GNAQ | IL12A | MKI67 | NTRK2 | SDHB | VCAM1 |
| AKT3 | CAD | CRKL | FANCA | GPI | IL12B | MLH1 | NTRK3 | SETD2 | VCP |
| ALDH1A1 | CBFB | CSF1R | FANCB | GSK3B | IRF1 | MPL | PALB2 | SHH | VEGFA |
| ALK | CCL2 | CSF3R | FANCC | GTSE1 | IRS2 | MS4A1 | PDCD1 | SMAD4 | VHL |
| AMER1 | CCL5 | CTLA4 | FANCD2 | GZMA | JAG1 | MSH2 | PDGFRA | SMO | VIM |
| APC | CCND1 | CTNNB1 | FANCF | GZMB | JAK1 | MSH6 | PDGFRB | SNAI1 | WNT1 |
| AR | CCND2 | CX3CL1 | FANCG | GZMH | JAK2 | MTOR | PIK3CA | SOX2 | WNT10A |
| ATAD2 | CCND3 | CXCL10 | FANCI | HBEGF | KDR | MYC | PIK3CG | SOX9 | WNT10B |
| ATM | CD22 | CXCL11 | FANCL | HDAC1 | KEAP1 | MYCN | PIK3R1 | SRC | WNT2B |
| ATR | CD274 | CXCL9 | FANCM | HDAC4 | KIT | MYD88 | PMS2 | STAT3 | WNT3 |
| AURKA | CD3D | CXCR3 | FAS | HES1 | KMT2A | NANOG | PRKCG | STAT6 | WNT4 |
| AXIN1 | CD4 | CXCR4 | FBXW7 | HGF | KRAS | NF1 | PRKCI | STK11 | WNT5A |
| AXIN2 | CD47 | DBF4 | FGF23 | HNF1A | LAG3 | NF2 | PTCH1 | SYK | WNT7A |
| AXL | CD68 | DDR2 | FGFR1 | HOXA9 | LNX2 | NFE2L2 | PTEN | TBX21 | WNT8A |

| | | | | | | | | | |
|-------|--------|-------|-------|--------|--------|--------|-------|---------|-------|
| BAP1 | CD79B | DOT1L | FGFR2 | HRAS | LYN | NFKBIA | RAB7A | TCF3 | WNT9A |
| BARD1 | CD8A | EGF | FGFR3 | ICAM1 | MAP2K1 | NGF | RAD50 | TCF4 | WNT9B |
| BCL2 | CDC7 | EGFR | FGFR4 | IDH1 | MAP2K2 | NGFR | RAD51 | TCF7L2 | WT1 |
| BCL6 | CDH1 | EP300 | FH | IDH2 | MAP2K4 | NKX2-1 | RAF1 | TGFA | XPO1 |
| BDNF | CDH2 | EPGN | FLT1 | IDO1 | MAPK1 | NOTCH1 | RALA | TGFBR2 | |
| BRAF | CDK4 | EPHA2 | FLT3 | IFNG | MAPK3 | NOTCH2 | RALB | TNFRSF4 | |
| BRCA1 | CDK6 | EPHA3 | FLT4 | IGF1 | MCL1 | NOTCH3 | RARA | TNIK | |
| BRCA2 | CDKN1B | ERBB2 | FOXP3 | IGF1R | MCM2 | NPM1 | RB1 | TOP1 | |
| BRD3 | CDKN2A | ERBB3 | GAS6 | IGF2 | MDM2 | NRAS | RET | TOP2A | |
| BRD4 | CEBPA | ERBB4 | GATA3 | IGF2R | MEN1 | NRG1 | RNF43 | TP53 | |
| BRDT | CHEK1 | EREG | GATA6 | IGFBP1 | MERTK | NTF3 | ROS1 | TSC1 | |

2 - Retrospective translational study of the Australian MAX trial, as previously described ³.

3 - Samples tested by Foundation Medicine were assayed with a validated comprehensive genomic profiling (CGP) platform during the course of clinical care at the request of the treating physician. DNA was extracted from 40 microns of FFPE sections, and CGP was performed on hybridization-captured, adaptor ligation based libraries to a mean coverage depth of >650X for 236 or 315 cancer-related genes plus select introns from 19 or 28 genes frequently rearranged in cancer as described previously ⁴. All classes of genomic alterations (GA) were identified including base pair substitutions, insertions/deletions, copy number alterations, and rearrangements. Microsatellite instable (MSI-H) or stable (MSS) status as a measure of mismatch repair deficiency was determined using a proprietary computational algorithm. Tumors were classified as microsatellite instable (MSI-H) or microsatellite stable (MSS) using a principal component 1 cutoff value of less than -8.5 or greater than -4, respectively ⁵.

4 - Samples tested by Memorial Sloan Kettering Cancer Center underwent analysis by the clinically validated MSK-IMPACT assay. This hybridization-based next generation sequencing assay interrogates all exons and select introns and promoters of over 340 cancer-related genes. Tumor samples are sequenced against matched normal samples and only somatic alterations including structural variants, mutations, and copy number alterations are reported. Further details about this assay have been published by Cheng et al. ⁶.

***In silico* analysis of the TCGA data (ALK, ROS1, NTRK fusion search in TCGA-COAD-READ)**

FPKM-normalized transcriptomic profiles were downloaded from the Genomic Data Commons Data Portal (<https://gdc-portal.nci.nih.gov>) for the tumor samples in the TCGA-COAD and TCGA-READ datasets and the z-score for each gene was calculated. Tumors in the 95th percentile for *ALK*, *NTRK1*, *NTRK2*, *NTRK3* or *ROS1* gene expression were selected for further analyses, since outlier

kinase expression is often driven by fusion transcripts^{7,8}. For the 154 tumor samples carrying outlier expression in one of the selected kinases (as shown in Supplementary Fig. 2 and listed in Supplementary Table 4), RNAseq reads were downloaded from the Genomic Data Commons Data Portal. Reads were aligned using the BWA-mem⁹ algorithm to hg19 human reference genome, then all the non-perfect alignments falling on the genes of interest were selected and aligned using BLAT¹⁰ with tileSize=11 and stepSize=5. The resulting alignment was post-processed to detect chimeric alignments, by applying the following criteria: i) each fusion partner must have at least 15 nucleotides mapped of the respective end of the read; ii) the two parts of the read must map to different genes; iii) at least one of the two fusion breakpoints must be on the exon boundary. Due to the short read length (ranging from 48 to 76, Supplementary Table 4), it was not possible to impose a threshold on the number of reads supporting each fusion breakpoint. After the first gene-specific analysis, we did a cross-validation on the entire transcriptome using FusionMap¹¹. In addition to the six fusion transcripts found on selected genes using our custom-built pipeline, FusionMap was able to identify also a previously reported VPS18-NTRK3 translocation¹².

Characterization of the novel *SCYL3-NTRK1* fusion

For Patient #13 harboring the novel fusion, *SCYL3-NTRK1*, a set of PCR primers was generated to further confirm the result (*SCYL3*: 5'- GGAGGAGAACGAACCAAGAT; *NTRK1*: 5'- CATGAAATGCAGGGACATGG). Total nucleic acid was reverse-transcribed and amplified by PCR using SuperScript III One-Step RT-PCR System with Platinum Taq High Fidelity (ThermoFisher, Carlsbad, CA). The PCR products were assessed on a 2100 Bioanalyzer electrophoresis system (Agilent, Santa Clara, CA). A parallel no template control was also included to determine the presence of any background hybridization.

Criteria for evaluation of primary resistance to anti-EGFR monoclonal antibodies

To assess the association of *ALK*, *ROS1* and *NTRK* status with primary resistance to anti-EGFR MoAbs, we restricted the analysis to *RAS* and *BRAF* wild-type patients receiving cetuximab or panitumumab as single agents or in combination with irinotecan, only in strictly defined irinotecan-refractory patients (i.e. those with documented disease progression during or within three months from the last irinotecan-containing therapy). We excluded patients receiving an anti-EGFR agent in combination with chemotherapy, except in the case of disease progression as best response indicating primary resistance to the whole treatment. Thus, we were able to focus on the true impact of *ALK*, *ROS1* and *NTRK* translocations on treatment resistance.

Supplementary Table S1. *ALK*, *ROS1*, *NTRK* rearranged cases described in the literature.

| Reference | <i>NTRK</i> fusions N=9 | <i>ALK</i> fusions N=13 | <i>ROS1</i> fusions N=2 | Retrieved case |
|---------------------------------|---|--|--|-------------------------------------|
| Lin et al, 2009 [2] | | <i>EML4-ALK</i> <i>EML4-ALK</i> | | No No |
| Lipson et al, 2012 [3] | | <i>C2orf44-ALK</i> | | No |
| Aisner et al, 2014 [4] | | <i>EML4-ALK</i> | <i>SLC34A2-ROS1</i> <i>Unknown-ROS1</i> | Yes Yes Yes |
| Houang et al, 2015 [5] | | <i>PPP1R21- ALK</i> | | No, stage II |
| Créancier et al, 2015 [6] | <i>TPR-NTRK1</i> <i>TPM3-NTRK1</i> | | | No, stage II No, stage II |
| Lee J et al, 2015 [6] | | <i>CAD-ALK</i> <i>EML4-ALK</i> | | Yes Yes |
| Sartore Bianchi et al, 2015 [7] | <i>LMNA-NTRK1</i> | | | Yes |
| Lee S et al, 2015 [8] | <i>TPM3-NTRK1</i> <i>TPM3-NTRK1</i> | | | Yes Yes |
| Amatu et al. 2015 [9] | | <i>CAD-ALK</i> | | Yes |
| Park et al. 2016 [10] | <i>LMNA-NTRK1</i> <i>TPM3-NTRK1</i> <i>TPM3-NTRK1</i> | | | No, stage II No, stage III No |
| Yakirevich et al. 2016 [11] | | <i>STRN-ALK</i> <i>CENPF-ALK</i> <i>MAPRE3-ALK</i> <i>EML4-ALK</i> <i>PRKAR1B- ALK</i> | | Yes Yes Yes Yes Yes |
| Hechtman et al. 2016 [12] | <i>ETV6-NTRK3</i> | | | Yes |

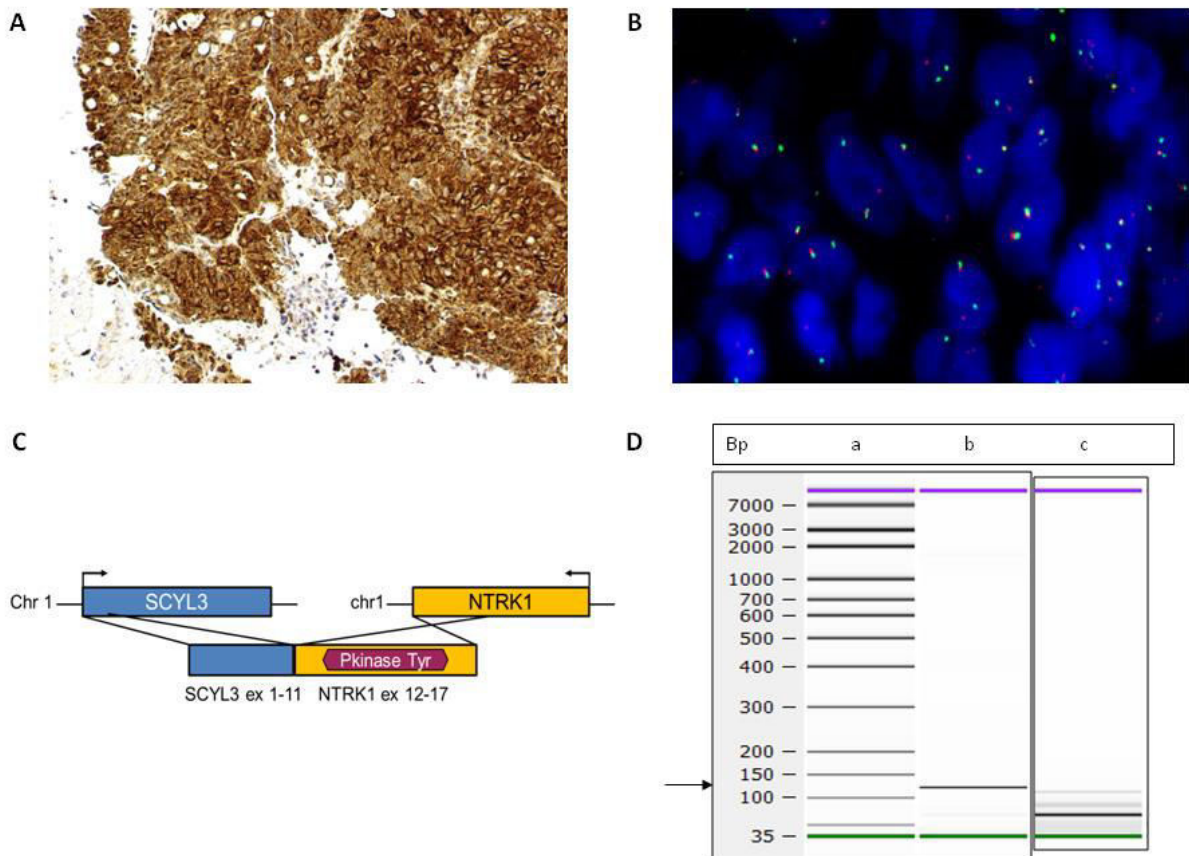
Supplementary Table S2. List of patients bearing *ALK*, *ROS1*, *NTRK* rearrangements with retrieving source, clinical center, identified gene fusion and NGS panel used.

| Patient | Retrieving source | Clinical center | Gene Fusion | NGS panel |
|----------------|------------------------------|-------------------------|---------------------|------------------|
| #1 | Ignyta Inc. | SMC, South Korea | <i>TPM3-NTRK1</i> | Minerva panel |
| #2 | Ignyta Inc. | SMC, South Korea | <i>EML4-ALK</i> | Minerva panel |
| #3 | Ignyta Inc. | SMC, South Korea | <i>TPM3-NTRK1</i> | Minerva panel |
| #4 | Foundation Medicine, MA, USA | SMC, South Korea | <i>CAD-ALK</i> | FMI panel |
| #5 | Foundation Medicine, MA, USA | MSKCC, NYC, USA | <i>ETV6-NTRK3</i> | FMI panel |
| #6 | MSKCC, NYC, USA | MSKCC, NYC, USA | <i>LMNA-NTRK1</i> | MSK-IMPACT |
| #7 | Foundation Medicine, MA, USA | MSKCC, NYC, USA | <i>LMNA-NTRK1</i> | FMI panel |
| #8 | Austin Health, Australia | MAX study Investigators | <i>C2orf44-ALK</i> | Minerva panel |
| #9 | Austin Health, Australia | MAX study Investigators | <i>Unknown-ROS1</i> | Minerva panel |
| #10 | Austin Health, Australia | MAX study Investigators | <i>SLC34A2-ROS1</i> | Minerva panel |
| #11 | Ignyta Inc. | NCC, Italy | <i>LMNA-NTRK1</i> | Minerva panel |
| #12 | Ignyta Inc. | NCC, Italy | <i>CAD-ALK</i> | Minerva panel |
| #13 | Ignyta Inc. | INT, Italy | <i>SCYL3-NTRK1</i> | Minerva panel |
| #14 | Ignyta Inc. | INT, Italy | <i>TPM3-NTRK1</i> | Minerva panel |
| #15 | Ignyta Inc. | UHG, Belgium | <i>EML4-ALK</i> | Minerva panel |
| #16 | Foundation Medicine, MA, USA | Unknown | <i>CENPF-ALK</i> | FMI panel |
| #17 | Foundation Medicine, MA, USA | Unknown | <i>PRKAR1B-ALK</i> | FMI panel |
| #18 | Foundation Medicine, MA, USA | Unknown | <i>TPM3-NTRK1</i> | FMI panel |
| #19 | Foundation Medicine, MA, USA | Unknown | <i>TPM3-NTRK1</i> | FMI panel |
| #20 | Foundation Medicine, MA, USA | Unknown | <i>EML4-ALK</i> | FMI panel |
| #21 | Foundation Medicine, MA, USA | Unknown | <i>TPM3-NTRK1</i> | FMI panel |

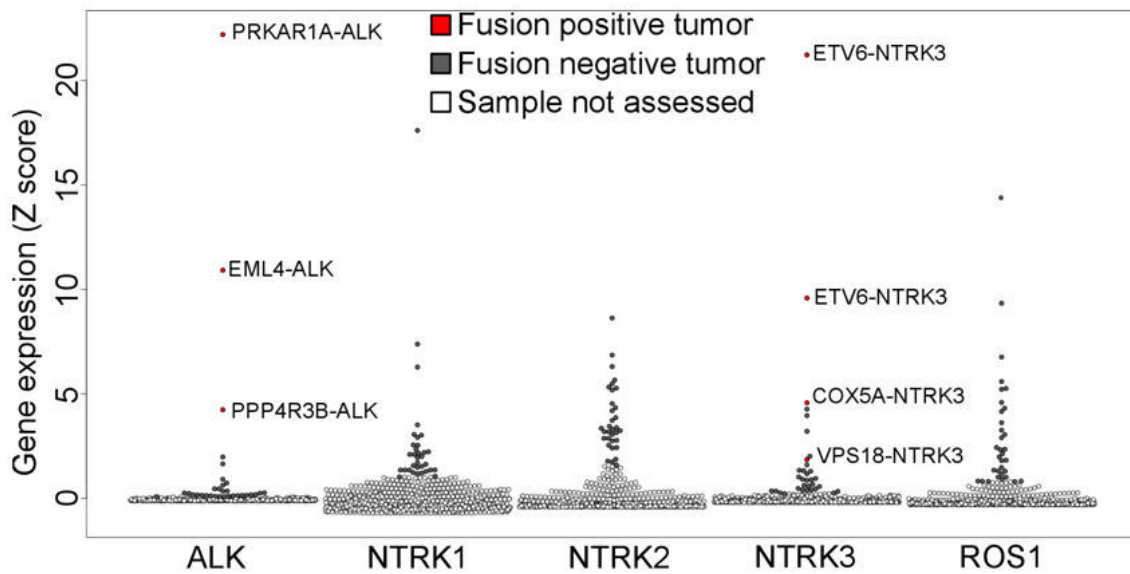
| | | | | |
|-----|------------------------------|---------|-------------------|-----------|
| #22 | Foundation Medicine, MA, USA | Unknown | <i>MAPRE3-ALK</i> | FMI panel |
| #23 | Foundation Medicine, MA, USA | Unknown | <i>STRN-ALK</i> | FMI panel |
| #24 | Foundation Medicine, MA, USA | Unknown | <i>CAD-ALK</i> | FMI panel |
| #25 | Foundation Medicine, MA, USA | Unknown | <i>TPM3-NTRK1</i> | FMI panel |
| #26 | Foundation Medicine, MA, USA | Unknown | <i>GOPC-ROS1</i> | FMI panel |
| #27 | Foundation Medicine, MA, USA | Unknown | <i>ETV6-NTRK3</i> | FMI panel |

Supplementary Figure 1. Identification and characterization of a novel *SCYL3-NTRK1* in a CRC sample.

Panel A: Immunohistochemistry (IHC) staining of tissue from Patient #13 using a cocktail of pan-Trk, ROS1 and ALK antibodies and a single DAB detection system. Strong staining intensity was seen in almost 100% of tumor nuclei indicating the elevated expression of at least one of the targeted proteins. **Panel B:** *NTRK1* FISH (Abnova SPEC NTRK1) was performed on the same specimen and resulted in break-apart positivity for the *NTRK1* gene in 100% of nuclei. **Panel C:** An RNA-based NGS assay using AMP-technology was performed to identify the fusion/fusion partner. This patient exhibited an intrachromosomal inversion and rearrangement that leads to a novel in-frame fusion of *SCYL3* exon 11 to exon 12 of *NTRK1* (upstream of the NTRK1 kinase domain in exons 13-17). **Panel D:** To confirm the novel fusion, RT-PCR was performed using primers specific to the *SCYL3-NTRK1* gene rearrangement. Lane a is a nucleic acid size ladder, annotated in base pair sizes by the column titled ‘Bp’; lane b is the RT-PCR product obtained from the patient specimen using rearrangement primers. The arrow indicates the specific RT-PCR product, which migrated at the expected 126 bp size; lane c is a no template control using the same primers as in lane b, which resulted in absence of a PCR product at the expected 126 bp (the strongest product generated migrates at 66 bp).

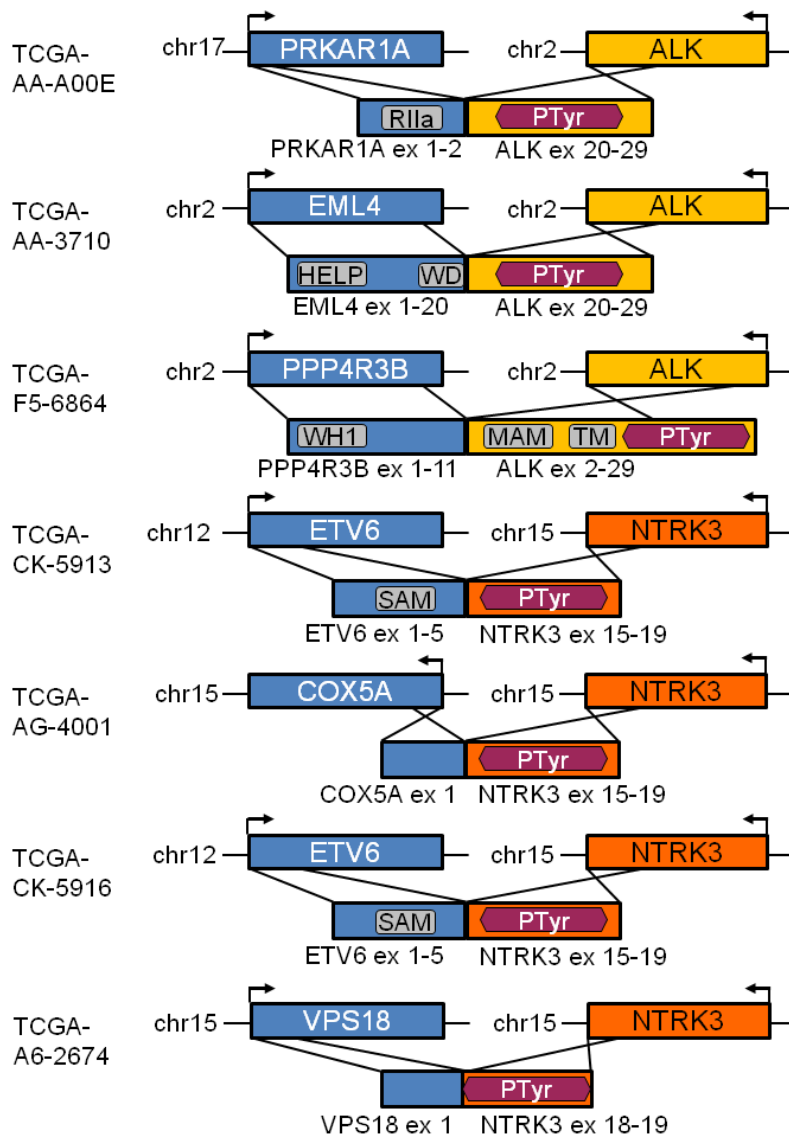


Supplementary Figure 2. Identification of gene fusions in TCGA colorectal cancer samples by outlier kinase analysis. Scatter-plot representation of transcriptional outlier kinases in TCGA CRC samples (N = 644). Grey coloured circles indicate 154 samples (listed in Supplemental Table S4) carrying outlier *ALK*, *NTRK1*, *NTRK2*, *NTRK3*, *ROS1* gene expression, defined as the 95th percentile for each gene based on z-score normalization. Gene fusion identification in the RNA sequencing reads from these 154 samples was performed by applying a custom pipeline (see Online Methods) and the FusionMap¹ algorithm. A total of 7 fusions (red circles) in the selected kinases were found.

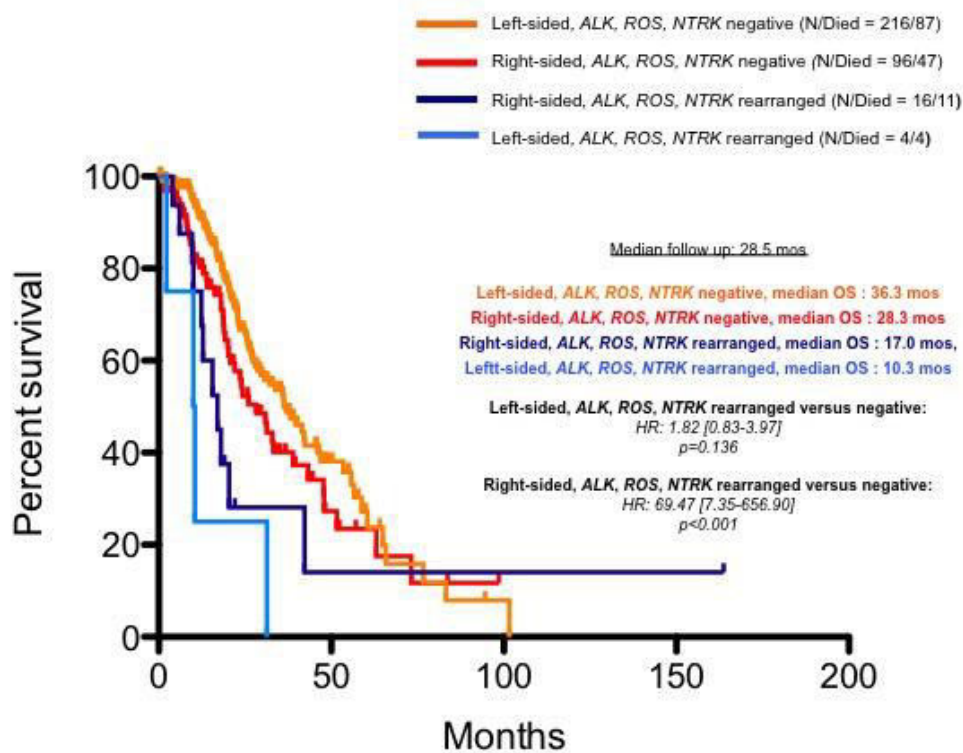


1. Ge, H., *et al.* FusionMap: detecting fusion genes from next-generation sequencing data at base-pair resolution. *Bioinformatics* 27, 1922-1928 (2011).

Supplementary Figure 3. Putative fusion diagrams for each TCGA CRC sample based on publicly available RNA sequencing data. All fusions include the ALK or NTRK3 full tyrosine kinase domain (shown in purple), with the exception of sample TCGA-A6-2674, in which only a portion of the kinase domain was retained. Genomic partner (depicted in blue) is on the left and tyrosine kinase receptor is on the right. Arrows indicate the direction of transcription for each gene. Chromosomes and exons (ex) are also indicated. 1, PRKAR1A–ALK fusion containing a portion of the PRKAR1A regulatory subunit of type II PKA R-subunit (RIIa). 2, EML4–ALK fusion containing the EML4 Hydrophobic EMAP-like protein (HELP) motif and a portion of the WD40 domain. 3, PPP4R3B–ALK fusion containing also the meprin/A5/mu (MAM) and the transmembrane (TM) domains of ALK. 4, ETV6–NTRK3 fusion. 5, COX5A–NTRK3 fusion. 6, ETV6–NTRK3 fusion. 7, VPS18–NTRK3 fusion, in which only a portion of the kinase domain of NTRK3 is retained. Other abbreviations are as follows: PP4R3B, protein phosphatase 4 regulatory subunit 3B; SAM, Sterile alpha motif (SAM)/Pointed domain; HELP, Hydrophobic EMAP-Like Protein motif WD, WD40 repeat (also known as the beta-transducin repeat); WH1, WASp Homology domain 1; MAM, meprin/A5/mu domain; TM, transmembrane domain.

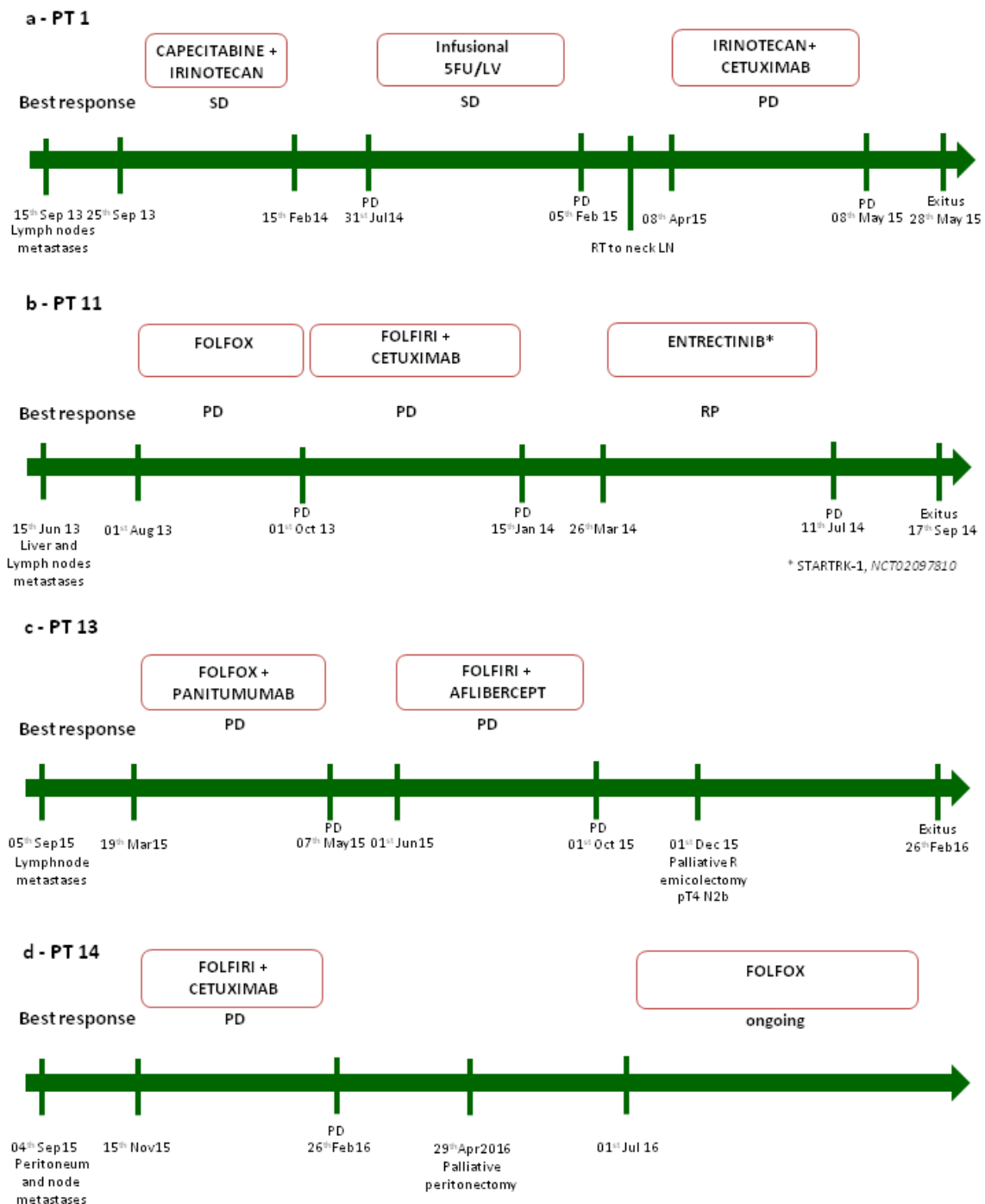


Supplementary Figure 4. Survival in metastatic colorectal cancer patients in subgroups defined by *ALK*, *ROS1*, *NTRK* rearrangements and primary tumor location. Kaplan-Meier curves for overall survival (OS) in patients with left-sided primary and *ALK*, *ROS1*, *NTRK* rearranged tumors (n=4; light blue line) as compared to those with left-sided primary and *ALK*, *ROS1*, *NTRK* negative tumors (n=216; orange line) and in patients with right-sided primary and *ALK*, *ROS1*, *NTRK* rearranged tumors (n=16; blue line) as compared to those with right-sided primary and *ALK*, *ROS1*, *NTRK* negative tumors (n=96; red line).

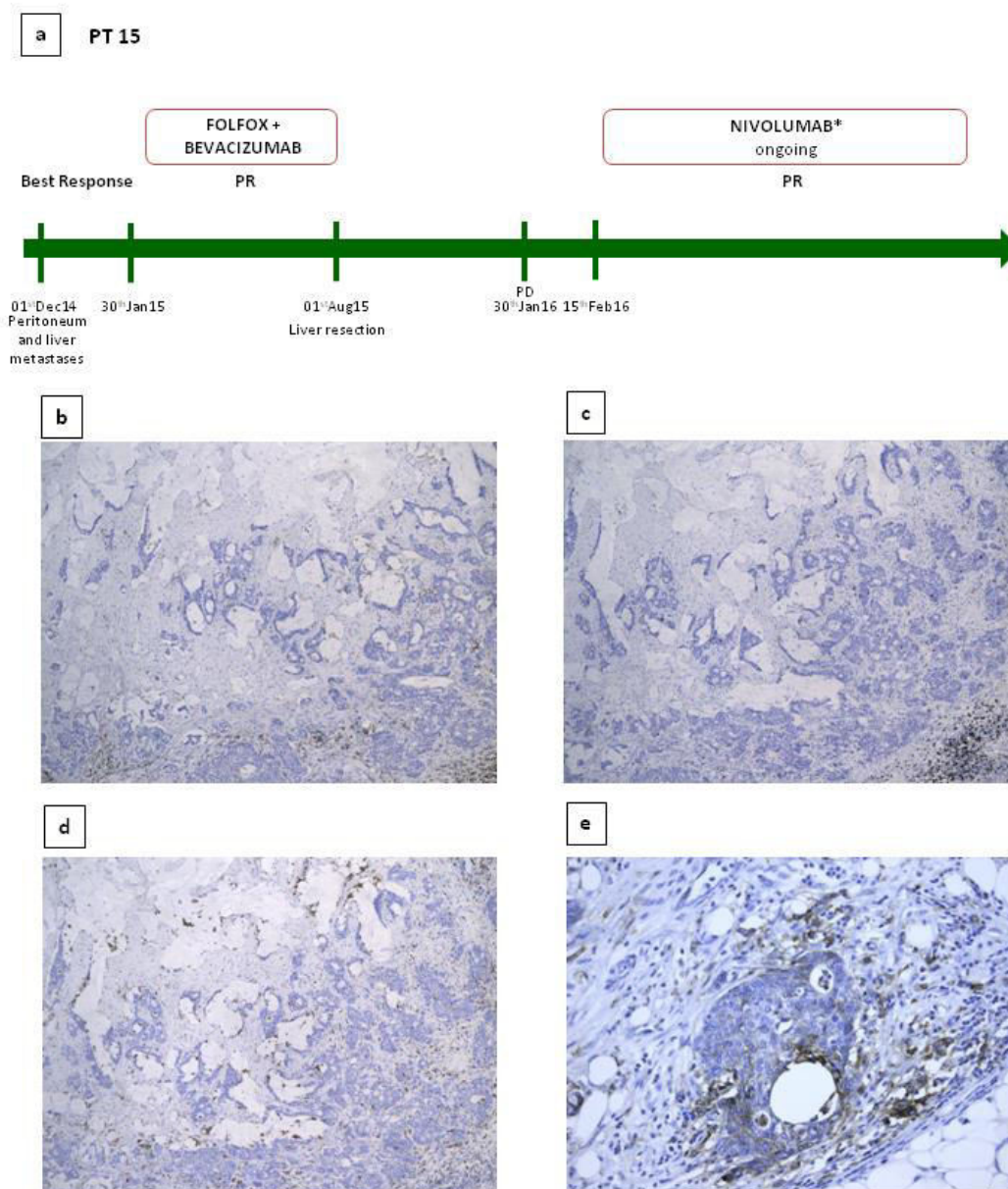


| | | | | | |
|--|-----|----|---|---|---|
| Left - <i>ALK</i> , <i>ROS</i> , <i>NTRK</i> neg. | 216 | 17 | 1 | 0 | 0 |
| Right - <i>ALK</i> , <i>ROS</i> , <i>NTRK</i> neg. | 96 | 8 | 1 | 0 | 0 |
| Right - <i>ALK</i> , <i>ROS</i> , <i>NTRK</i> rearr. | 16 | 2 | 2 | 1 | 0 |
| Left - <i>ALK</i> , <i>ROS</i> , <i>NTRK</i> rearr. | 4 | 0 | 0 | 0 | 0 |

Supplementary Figure 5. Summary of the clinical history of the four patients (N°1, 11, 13 and 14) evaluable for response to anti-EGFR monoclonal antibodies (cetuximab or panitumumab). Shaded boxes indicate periods of administration of the indicated chemotherapeutic agents. Blue vertical lines indicate timing of tumor specimen acquisition from surgical procedures or biopsy, as well as dates of tumor assessment by radiological imaging. As shown, all evaluable patients had progressive disease to anti-EGFR-based therapy.



Supplementary Figure 6. Summary of the clinical history and immunohistochemical study of the patient (N°15) responding to immune checkpoint inhibition. Panel A. Summary of the clinical history of the patient with EML4-ALK fusion and MMR deficient status (N°15) receiving anti-PD-1 immunotherapy with nivolumab. Shaded boxes indicate periods of administration of the indicated chemotherapeutic agents. Blue vertical lines indicate timing of tumor specimen acquisition from surgical procedures or biopsy, as well as dates of tumor assessment by radiological imaging. As shown, the patients had partial response to anti-PD-1 which is still ongoing. **Panel B.** Positive immunohistochemical staining for CD4. **Panel C.** Positive immunohistochemical staining for CD8. **Panel D.** Positive immunohistochemical staining for CD68. **Panel E.** Positive immunohistochemical staining for PD-L1 in >50% of tumor cells.



Supplementary References

- 1 Murphy DA, Ely HA, Shoemaker R., et al. Detecting Gene Rearrangements in Patient Populations Through a 2-Step Diagnostic Test Comprised of Rapid IHC Enrichment Followed by Sensitive Next-Generation Sequencing. *Appl Immunohistochem Mol Morphol* 2016; <https://dx.doi.org/10.1097/PAI.0000000000000360> published online Mar 29.
- 2 Zheng Z, Liebers M, Zhelyazkova B, et al. Anchored multiplex PCR for targeted next-generation sequencing. *Nat Med* 2014;20:1479-84.
- 3 Tebbutt NC, Wilson K, GebSKI VJ, et al. Capecitabine, bevacizumab, and mitomycin in first-line treatment of metastatic colorectal cancer: results of the Australasian Gastrointestinal Trials Group Randomized Phase III MAX Study. *J Clin Oncol* 2010;28:3191-8.
- 4 Frampton GM, Fichtenholtz A, Otto GA, et al. Development and validation of a clinical cancer genomic profiling test based on massively parallel DNA sequencing. *Nat Biotechnol* 2013; 31:1023-31.
- 5 Hall, M.J., et al. Evaluation of microsatellite instability (MSI) status in gastrointestinal (GI) tumor samples tested with comprehensive genomic profiling (CGP). *J Clin Oncol* 2016; 34 (suppl 4S) abstr 528.
- 6 Cheng DT, Mitchell TN, Zehir A, et al. Memorial Sloan Kettering-Integrated Mutation Profiling of Actionable Cancer Targets (MSK-IMPACT): A Hybridization Capture-Based Next-Generation Sequencing Clinical Assay for Solid Tumor Molecular Oncology. *J Mol Diagn* 2015;17:251-64.
- 7 Kothari V, Wei I, Shankar S, et al. Outlier kinase expression by RNA sequencing as targets for precision therapy. *Cancer Discov* 2013;3:280-93.
- 8 Medico E, Russo M, Picco G, et al. The molecular landscape of colorectal cancer cell lines unveils clinically actionable kinase targets. *Nat Commun* 2015;6:7002.
- 9 Li H, Durbin R. Fast and accurate long-read alignment with Burrows-Wheeler transform. *Bioinformatics* 2010;26:589-95.
- 10 Kent WJ. BLAT--the BLAST-like alignment tool. *Genome Res* 2002; 12:656-64.
- 11 Ge H, Liu K, Juan T, Fang F, Newman M, Hoek W. FusionMap: detecting fusion genes from next-generation sequencing data at base-pair resolution. *Bioinformatics* 2011;27:1922-8.
- 12 Yoshihara K, Wang Q, Torres-Garcia W, et al. The landscape and therapeutic relevance of cancer-associated transcript fusions. *Oncogene* 2015;34:4845-54.